Supporting Information

Jacobs et al. 10.1073/pnas.0911213107

SI Results

We performed a series of follow-up analyses to further examine the properties of the 30 clockwise and counterclockwise path cells and to test alternate explanations for their activities. As mentioned previously, one potential explanation for apparant clockwise or counterclockwise path-cell activity is that these cells are actually responding to right or left turns. For example, right turns are prevalent in clockwise paths, so a "right turn" cell (1) might appear as a clockwise path cell. To investigate the potential relation between path cells and turning, we examined neuronal activity when patients veered toward the outside of the environment while driving (i.e., left turning during clockwise movement and right turning during counterclockwise movement). These outward turns can occur when a patient swerves to reach a destination store on the environment's outer wall, or when the patient begins a "U" turn. Analyzing neuronal activity here allows us to distinguish which factor better predicts path-cell firing: the clockwise or counterclockwise direction of movement, or the right or left direction of a turn. For example, a true clockwise path cell should have a greater firing rate during outward left turns at clockwise headings than during outward right turns at counterclockwise headings, whereas a right-turn cell would show the opposite pattern. We found that path cells were significantly more active during outward turns in their preferred direction than during outward turns in their nonpreferred direction (one-sided sign-rank test, $P < 10^{-4}$). This indicates that path-cell activity is most closely related to the overall clockwise or counterclockwise direction of movement, rather than to the instantaneous direction of a turn.

To further examine whether path-cell responses were related to turning, we separately analyzed the activity of each path cell in "straightaways," defined as epochs when the patient was driving straight (i.e., not turning) through noncorner sections of the virtual environment. Then we compared the firing rate of each path cell between straightaways in the cell's preferred direction (clockwise or counterclockwise) and straightaways in the nonpreferred direction. If path cells were truly encoding the overall direction of movement, then we expected that robust directional activity would appear during these straightaways. On the other hand, if path cells were encoding turn-related activity, then no direction-specific activity should appear during straightaways. This comparison revealed that path cells had significantly higher firing rates during straightaways in their preferred direction than in straightaways in their nonpreferred direction (one-sided sign-rank test, $P < 10^{-6}$). This indicates that path cells encode directional information that is not directly related to turning.

Another potential explanation for the behavior of path cells is that these cells are actually encoding the right or left direction of a *future* or *past* turn. Indeed, recent studies showed that rodent EC neurons performed this prospective coding (encoding future locations or events) or retrospective coding (encoding past locations or events) (2, 3), and one path cell in our dataset appeared to have an especially elevated firing rate when approaching a clockwise turn (Fig. 2*C*). To test whether path-cell activity was consistent with prospective coding, we separately analyzed each path cell's activity in the final, straight approach to the destination store (i.e., after leaving the corner of the environment; Fig. S3*A*). During this final approach, the patient is driving directly to the intended destination, where they will deliver their passenger and then make a pause before the next delivery. In this interval they have no information regarding future, postdelivery turns and thus neuronal activity here is not likely to be related to prospective coding of an upcoming turn. We calculated the firing rate of each path cell during this final approach and found that this activity was consistent with path cells' overall clockwise or counterclockwise preferred directions (one-sided sign-rank test, $P < 10^{-5}$; Fig. S3*B*). Thus, it appeared that path cells still encoded their preferred direction even after accounting for the potential influence of prospective coding. We also conducted an analogous analysis to test whether retrospective coding could account for our results. To do this, we examined neuronal activity at the beginning of each delivery before reaching the environment's corner (Fig. S3*C*). Again, we found that path cells significantly encoded their preferred direction during this period (one-sided sign-rank test, $P < 10^{-5}$), indicating that retrospective coding does not account for the path-cell activity we observed. Based on these analyses, it appears that clockwise and counterclockwise path-cell activity reflects a different phenomenon than prospective or retrospective coding.

One interesting question is whether path-cell directional activity is immediately present when the task begins or whether it emerges only after significant exposure to the environment. For example, if path-cell directional activity was related to an order-dependent memory of the environment's layout, these patterns might appear only after the environment's landmarks were well learned. To examine this, we studied path-cell directional activity in the first delivery of each testing session, before the environment's layout was learned. Including only sessions where patients drove in both clockwise and counterclockwise directions during the first delivery, we found that path cells were more active during movements in their preferred direction than during movements in their nonpreferred direction (one-sided t test, $P < 0.08$). This suggests that path-cell directional responses were present immediately upon entering the environment and thus it seems unlikely that they encoded memory for spatial landmarks.

Although many electrophysiological studies of spatial navigation focus on excitatory cells, in recent literature the functional role of interneurons has received increased interest. Historically, interneurons were often excluded from navigation studies because they did not show a clear relation to spatial navigation (4). However, recent studies that used more sensitive statistical techniques found that some interneurons robustly encoded location-related information (5, 6). In our dataset, 9.3% of all neurons were putative interneurons (*Materials and Methods*). To test for potential differences in the properties of interneuron and noninterneuron path cells, we separately compared the spatial coding properties of interneuron and noninterneuron EC path cells. We found that these two groups did not significantly differ in terms of either A_{dir} or D_{pref} (two-sided rank-sum tests, both P values >0.2). Because we did not observe any significant differences between these cell classes, we pooled both groups for statistical analyses. In addition to path cells, we also examined the prevalence of place cells among interneurons. However, in this dataset we did not observe significant levels of place cells among interneurons (binomial test, $P > 0.6$).

SI Discussion

In addition to spatial information, EC neurons encode various types of nonspatial variables (7–9). Thus, neurons that appear as path cells during navigation might also be involved in coding different types of information in nonspatial tasks. Path cells' encoding of clockwise or counterclockwise paths during navigation may be one example of a more general phenomenon in which EC neurons encode various characteristics of the current behavioral context. Unfortunately, because our dataset is limited to a spatial task, we are unable to directly examine how path cells behave during nonspatial tasks. Therefore, although our findings indicate

that the human EC has an important role in spatial cognition, they do not address the broader issue concerning the function of the EC in other behaviors.

One potential alternate explanation for the apparent clockwise- or counterclockwise-selective activity of path cells is that these neurons could be encoding a different event that is correlated with the clockwise or counterclockwise direction of movement. For example, during clockwise movement, patients might consistently tilt their eyes or head leftward to view the outer wall of the environment, which appears on the left side of the screen. This type of phenomenon could even occur in a subtle manner that does not involve any visible movement, for example, if patients merely shifted their attention to the left hemifield during clockwise travel without actually moving their eyes. If this type of direction-related behavior occurred, then a head-direction or spatial-attention cell (10, 11) could appear as a path cell. To address this type of issue, a future study will need to simultaneously record head and eye movements as neuronal activity is recorded from a patient performing the task, and also include a task manipulation that explicitly decorrelates movement direction from the location of visual attention.

It has been demonstrated in rodents that the position of a neuron along the dorsal–ventral axis of the EC is directly proportional to the distance (in space) between a grid cell's firing fields (12) and to the period of subthreshold membrane oscillations (13). If similar patterns exist in humans, then EC path cells at different anatomical locations might also systematically vary in their properties. Unfortunately, we were unable to examine this issue here, because standard clinical imaging does not provide sufficiently detailed information on each recording electrode's position. Examining how neuronal activity varies throughout the EC is an important topic for future research. However, it is not immediately clear to us how a continuous measure (dorsal–ventral anatomical distance) might relate to the activity of a neuron that appears to encode one of two discrete directions.

We note that Hough and Bingman (14) reported neurons in the pigeon hippocampus that they also identified with the term "path cells" because they exhibited elevated firing throughout large subregions ("paths") of the constrained environment, similar to place cells with especially large place fields. The directional properties of these pigeon path cells were not reported, and thus Hough and Bingman's findings qualitatively differ from the path cells that we described.

SI Materials and Methods

Behavioral Task. At the beginning of the first testing session, patients completed a short four-delivery practice session to familiarize them with the navigation controls. The practice environment was configured differently from the main task, and had four stores arranged in a large, wide-open arena. We did not analyze the data from this practice session. After the practice session, patients participated in the main task.

In the main task, the size of the virtual environment was 100 × 100 VR units, the width of the road was 25 VR units, and the obstructed area in the center of the road was 50 × 50 VR units. (As a result of this obstruction, we found that patients indeed drove in a clockwise or counterclockwise direction >99% of the time, excluding store approaches). The "corner" regions of the environment consisted of the four 25 × 25 VR-unit regions where roads intersected at 90° angles (shaded regions in Fig. S3*A*). During navigation, patients had a 60° field of view. Patients pushed the joystick forward to accelerate forward (maximum forward speed = 12.5 VR units/s) and pulled the joystick back to accelerate backward (maximum backward speed = 5 VR units/s). The patients could turn by pushing the joystick left or right (maximum angular velocity = 40°/s). To encourage patients to take the shortest route to each destination, patients received 50 points for each successful delivery and had one point deducted for each second that they spent navigating. The running point count was displayed on-screen at all times and patients were verbally instructed to maximize their point total.

Electrophysiology. Electrode locations were planned by clinical teams to map the seizure focus for potential subsequent resective surgery. Thus, the planned recording sites were distributed across widespread brain regions [1,419 total neurons: 301 in hippocampus, 176 in entorhinal cortex (EC), 93 in parahippocampal gyrus, 270 in amygdala, 335 in frontal cortex, and 244 in temporal and parietal cortices]. Because of limitations of the clinical testing environment, we were unable to localize each electrode to a specific subregion of each brain area. We used the clustering method of Viskontas et al. (15) to identify interneurons, using waveform shape, mean firing rate, and interspike intervals. We found that 9.9% of all cells were putative interneurons (hippocampus, 10%; EC, 14%; parahippocampal gyrus, 3.2%; amygdala, 5.9%; frontal cortex, 6.9%; temporal and parietal cortex, 15%). To visually depict the location of the right EC neurons from patient 2 (Fig. 2 *A*–*C*), we studied a computed tomographic image taken after electrode implantation and superimposed the electrode's location onto a preoperative magnetic resonance image (Fig. S1).

Data Analysis. We defined path cells as neurons that exhibited direction-related activity throughout large areas of the environment. To identify this phenomenon quantitatively, first, at each location we measured whether each neuron was active at a significantly different rate depending on whether the patient was moving clockwise or counterclockwise. This analysis was conducted separately at each location in a 100 × 100 VR-unit grid across the virtual environment. At each location, we identified all nearby epochs as those occurring within 10 VR units of that location. (This aggregation was necessary because our recordings are relatively short, compared with studies in animals, because of our clinical testing environment. We experimented with various forms of spatial binning, and found that this scale behaved optimally for these data.) If there were at least 10 nearby clockwise epochs and at least 10 nearby counterclockwise epochs, we then used a two-tailed Wilcoxon rank-sum test to compare the firing rates between these two sets of epochs. A neuron was determined to exhibit a significant effect of directionality at that location if this test indicated that the median firing rate significantly differed between these distributions ($P < 0.01$). We discarded epochs when the patient was not driving clockwise or counterclockwise (e.g., if patients were facing the outer wall while turning around) or when their speed was <5 VR units/s. Patients were considered to be turning if their angular velocity exceeded 15°/s. When patients' velocity, direction, or turn status changed in the middle of an epoch, we labeled such epochs with the most frequent value of the variable during the epoch.

Next, to summarize the areal extent of each cell's directional activity, we computed A_{dir}, which is the fraction of locations in the environment that exhibited significant directionality, out of all locations that were traversed in both directions. We used a reshuffling procedure to estimate the distribution of A_{dir}*, a random variable that we created to indicate the fraction of spatial locations at which this cell would exhibit significant directional activity by chance. To perform this reshuffling, we randomly time-shifted the neural firing rates relative to the behavioral epochs and computed A_{dir}* on the reshuffled dataset; this was repeated 100 times. This reshuffling procedure is important because it estimates the prevalence of spurious directional activity that could appear as a result of temporal correlations in a neuron's spike train or in the patient's behavior. We determined whether each neuron was a path cell by comparing the distribution of A_{dir}* estimated via the reshuffling procedure with the actual value of A_{dir}. A neuron was considered to be a path cell if A_{dir} exceeded the 95th percentile of A_{dir}* (i.e., $P < 0.05$). Furthermore, we established the additional criterion that A_{dir} must be >0.1 for a cell to be considered a path cell, to

ensure that a bona fide path cell exhibited directional activity throughout a large fraction of the environment.

We identified a set of path cells that had a consistent clockwise or counterclockwise directional preference across nearly all of the locations that exhibited significant directional activity (Fig. 2). To measure this phenomenon, we first identified the preferred clockwise or counterclockwise direction of each path cell (i.e., the direction that exhibited elevated neuronal activity across a larger area of the environment). Then we calculated D_{pref}, which is the fraction of spatial locations that had a significant preference for the preferred direction, out of all locations that exhibited a significant directional effect in either direction. D_{pref} varies between 0.5 (half of significantly directional locations are clockwise, half are counterclockwise) and 1 (all significantly directional locations are in the preferred direction). We also measured the directional information encoded by each cell via a directionality index. We computed this index by identifying the location where each neuron's activity exhibited the largest difference between clockwise and counterclockwise movements (i.e., the place field for place cells), and then performing a rank-sum test to compare the activity at this location between clockwise and counterclockwise movement. Each cell's directionality index was taken as the absolute value of the inverse-normal transformed P value from this test.

We were also interested in identifying place cells (16). In contrast to our path-cell analyses, where we identified cells with large areas of directional activity, here we aimed to find specific locations where the cell's firing rate significantly increased. Thus, each place cell encodes the patient's presence at this virtual location (the cell's "place field"). To do this, we used a statistical criterion such that each place cell must have at least one set of contiguous spatial locations where the cell's firing rate is significantly elevated compared with the baseline firing rate in the rest of the virtual environment. At each location across the environment, we used a one-sided rank-sum test to compute the probability P_{place} that the firing rate at nearby locations (distance $\leq$ 10 VR units) was significantly greater than the firing rate at distant locations (> 10 VR units). Thus, P_{place} essentially measures the information that the neuron encodes about each location. We conducted separate analyses for clockwise and counterclockwise place fields because previous work identified unidirectional place fields in rodents performing directionally organized tasks (17–20). (We also conducted a separate, unsuccessful search for omnidirectional place cells.) We assessed the statistical significance of each place field via 100 iterations of a time-shifting permutation procedure (detailed above). Using these randomly shuffled datasets, we estimated the distribution of $P^*_{first\_field}$, which is the smallest P threshold yielding at least one place field by chance. (Here we defined a place field as a contiguous region of $\geq$2% of the environment that exhibited significantly increased spiking activity compared with distant locations, according to a one-sided rank-sum test.) We then identified the fifth percentile of $P^*_{first\_field}$ and used it as the threshold for assessing statistical significance based on the values of P_{place} from the original dataset. This reshuffling procedure ensured that the Type 1 error rate for identifying a place cell in the original dataset was fixed at 5%.

1. Sato N, Sakata H, Tanaka Y, Taira M (2006) Navigation-associated medial parietal neurons in monkeys. *Proc Natl Acad Sci USA* 103:17001–17006.
2. Frank LM, Brown EN, Wilson M (2000) Trajectory encoding in the hippocampus and entorhinal cortex. *Neuron* 27:169–178.
3. Lipton PA, White JA, Eichenbaum H (2007) Disambiguation of overlapping experiences by neurons in the medial entorhinal cortex. *J Neurosci* 27:5787–5795.
4. Christian E, Deadwyler S (1986) Behavioral functions and hippocampal cell types: Evidence for two nonoverlapping populations in the rat. *J Neurophysiol* 55:331–348.
5. Ego-Stengel V, Wilson M (2007) Spatial selectivity and theta phase precession in CA1 interneurons. *Hippocampus* 17:161–174.
6. Wilent W, Nitz D (2007) Discrete place fields of hippocampal formation interneurons. *J Neurophysiol* 97:4152–4161.
7. Suzuki WA, Miller EK, Desimone R (1997) Object and place memory in the macaque entorhinal cortex. *J Neurophysiol* 78:1062–1081.
8. Charles DP, Browning PGF, Gaffan D (2004) Entorhinal cortex contributes to object-in-place scene memory. *Eur J Neurosci* 20:3157–3164.
9. Hargreaves E, Rao G, Lee I, Knierim J (2005) Major dissociation between medial and lateral entorhinal input to dorsal hippocampus. *Science* 308:1792–1794.
10. Blair HT, Sharp PE (1995) Anticipatory head direction signals in anterior thalamus: Evidence for a thalamocortical circuit that integrates angular head motion to compute head direction. *J Neurosci* 15:6260–6270.
11. Desimone R, Duncan J (1995) Neural mechanisms of selective visual attention. *Annu Rev Neurosci* 18:193–222.
12. Hafting T, Fyhn M, Molden S, Moser MB, Moser EI (2005) Microstructure of a spatial map in the entorhinal cortex. *Nature* 436:801–806.
13. Giocomo L, Zilli E, Fransen E, Hasselmo M (2007) Temporal frequency of subthreshold oscillations scales with entorhinal grid cell field spacing. *Science* 315:1719–1722.
14. Hough G, Bingman V (2004) Spatial response properties of homing pigeon hippocampal neurons: Correlations with goal locations, movement between goals, and environmental context in a radial-arm arena. *J Comp Physiol A* 190:1047–1062.
15. Viskontas I, Ekstrom A, Wilson C, Fried I (2007) Characterizing interneuron and pyramidal cells in the human medial temporal lobe in vivo using extracellular recordings. *Hippocampus* 17:49–57.
16. O'Keefe J, Dostrovsky J (1971) The hippocampus as a spatial map. Preliminary evidence from unit activity in the freely-moving rat. *Brain Res* 34:171–175.
17. McNaughton BL, Barnes CA, O'Keefe J (1983) The contributions of position, direction, and velocity to single unit activity in the hippocampus of freely-moving rats. *Exp Brain Res* 52:41–49.
18. Muller R, Bostock E, Taube J, Kubie J (1994) On the directional firing properties of hippocampal place cells. *J Neurosci* 14:7235–7251.
19. Markus EJ, et al. (1995) Interactions between location and task affect the spatial and directional firing of hippocampal neurons. *J Neurosci* 15:7079–7094.
20. Buzsáki G (2005) Theta rhythm of navigation: Link between path integration and landmark navigation, episodic and semantic memory. *Hippocampus* 15:827–840.
21. Doeller CF, Barry C, Burgess N (2010) Evidence for grid cells in a human memory network. *Nature* 463:657–661.

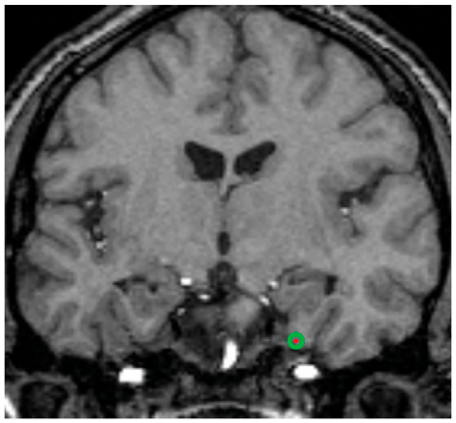

Fig. S1. Location of microelectrode bundle in patient 2's right entorhinal cortex. Brain image in neurological convention (i.e., right side of image depicts the right brain hemisphere). This electrode bundle appears to be in a region that is homologous to the rodent medial entorhinal cortex (21).

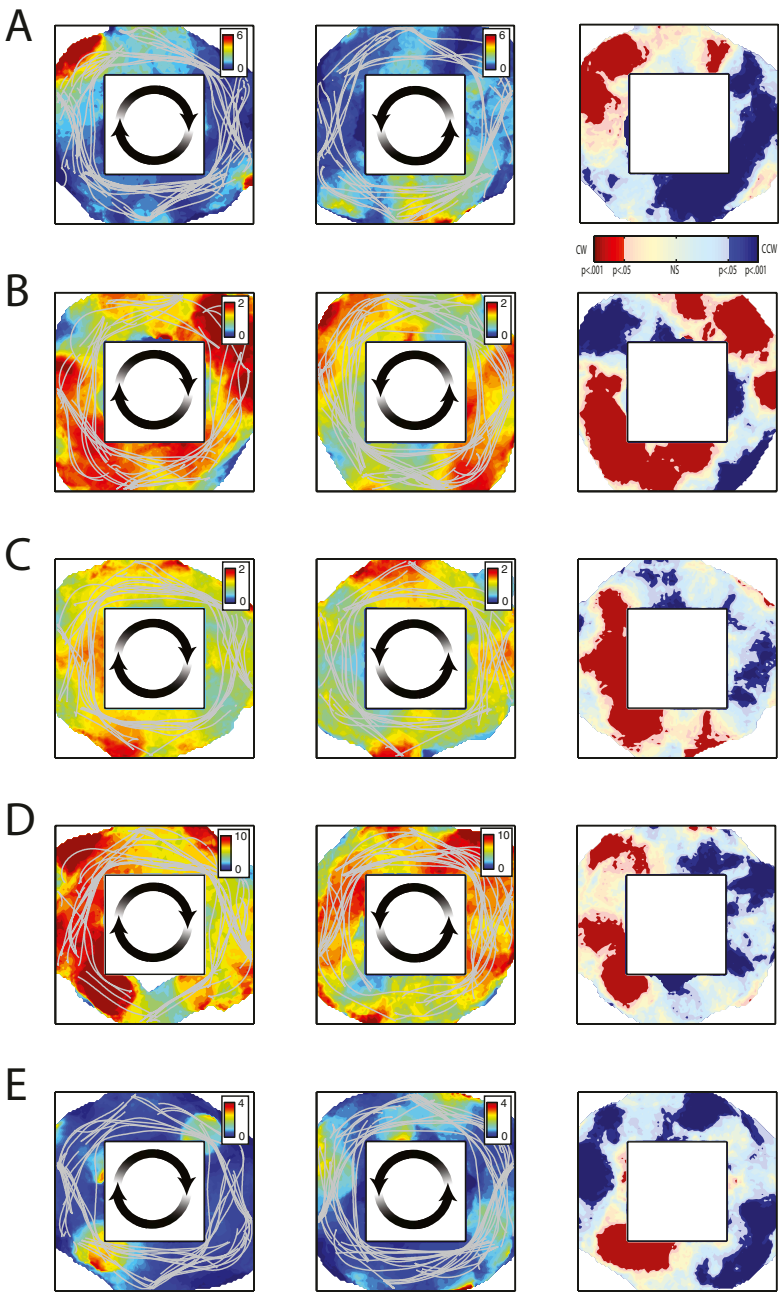

Fig. S2. Example complex path cells. These cells all exhibited significant directional firing across various locations in the environment, but there was not a single clockwise or counterclockwise preferred direction (Fig. 2). (*A*) Behavior of a path cell from patient 5′s left entorhinal cortex; (*Left*) this cell's activity during clockwise movements; (*Middle*) activity during counterclockwise movements. Gray lines indicate the path of the subject. (*Right*) Representation of whether firing rate at each location was statistically greater (rank-sum test) during clockwise movements (red) or during counterclockwise movements (blue). (Spatial statistics: A_{dir} = 0.32 and D_{pref} = 0.61; *Materials and Methods*). (*B*) Behavior of a path cell from patient 2's right entorhinal cortex. (A_{dir} = 0.46 and D_{pref} = 0.76.) (*C*) Behavior of a path cell from patient 4's right entorhinal cortex. (A_{dir} = 0.22 and D_{pref} = 0.94.) (*D*) Behavior of a path cell from patient 6's left entorhinal cortex. (A_{dir} = 0.19 and D_{pref} = 0.71.) (*E*) Behavior of a path cell from patient 2's right entorhinal cortex. (A_{dir} = 0.27 and D_{pref} = 0.69.)

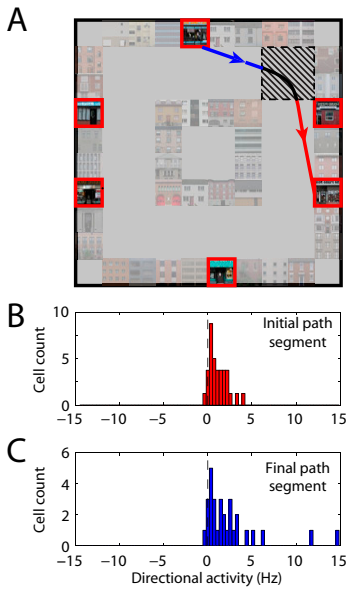

Fig. S3. Analysis of retrospective and prospective coding as an explanation for path-cell activity. (*A*) Overhead map of the environment, superimposed with an example path. Blue portion of path indicates the initial path segment that is analyzed in our retrospective-coding analysis; red portion of path indicates the final path segment analyzed in our prospective-coding analysis. Black cross-hatched region indicates the corner turn region of the environment. (*B*) Histogram of mean path-cell directional firing during the initial path segment. The median of this distribution (0.9 Hz) is significantly greater than 0 (sign-rank test, $P < 10^{-5}$). (*C*) Histogram of mean path-cell directional firing during the final path segment (median = 1.6 Hz; sign-rank test, $P < 10^{-5}$).

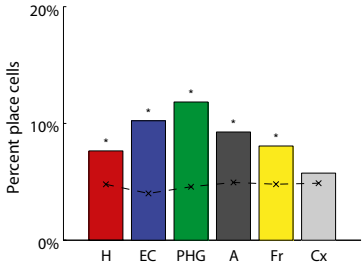

Fig. S4. Regional distribution of place cells. Bars depict percentages of neurons in each region that were place cells (cell counts in each region given in *Materials and Methods*). Abbreviations and color scheme are the same as in Fig. 3. Black dashed line and letter x indicates the percentages of path cells expected by chance. Asterisks indicate regions in which the number of observed path cells significantly exceeds the number expected by chance (binomial test, $P < 0.05$).

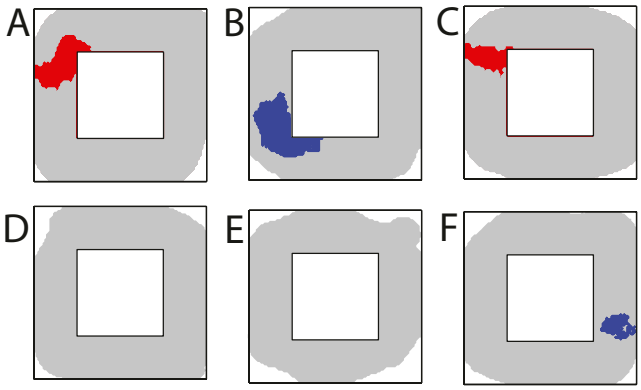

Fig. S5. Analysis of place fields in path cells. Results of applying our place-field analysis to the path cells the activities of which were illustrated in Fig. 2. (Each panel represents the cell from the corresponding panel in Fig. 2). The format for these plots follows the right column of Fig. 4.

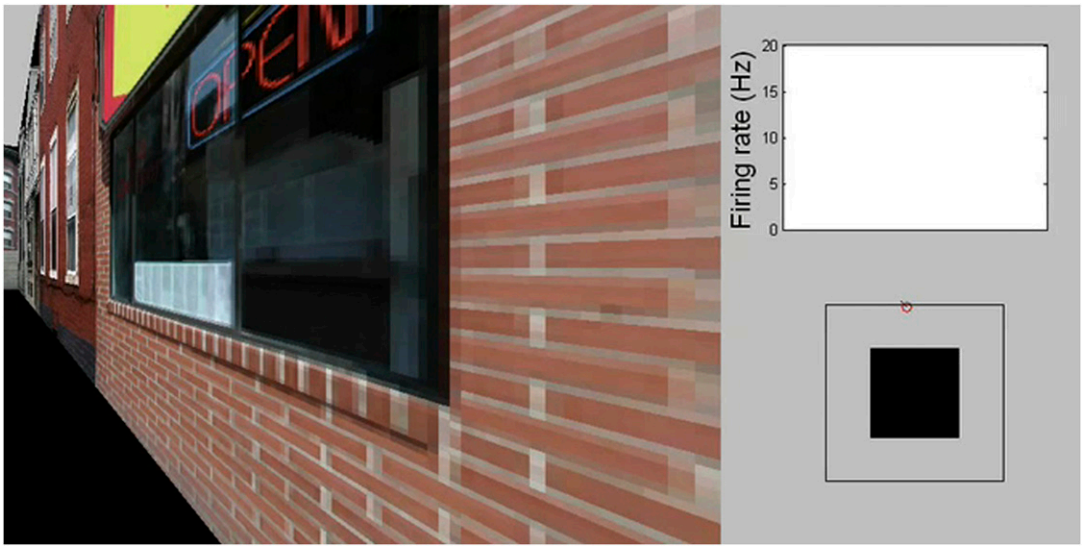

Movie S1. Activity of one example path cell. Movie depicts the activity of the path cell from Fig. 2*A* during part of the testing session. (*Left*) Computer reconstruction of the subject's view of the virtual town. (*Top right*) Smoothed firing rate of this cell. (*Bottom right*) Patient's current virtual location on an overhead view of the environment. Tick sounds in the movie's audio indicate when spikes occurred.

Movie S1